

On the role of GABAergic synapses in synchronization

Ho Young Jeong* and Boris Gutkin

*Gatsby Computational Neuroscience Unit, Alexandra House,
17 Queen Square, London WC1N 3AR, United Kingdom*

GABAergic synapses play an important role in the control of neural activity as well as the formation of neural circuitry. In particular, the reversal potential of GABAergic synapses can change significantly during development along with the intrinsic neuronal properties. In this report, we study the influence of such synaptic changes on synchrony in neural circuits. We use phase reduction methods to study the stability of synchrony. Numerical simulations of a conductance-based model based on the analysis exhibit the various firing conditions. We also extend the analysis to large globally coupled neuronal networks.

Keywords: synchronization, GABAergic synapses, Afterhyperpolarization

I. INTRODUCTION

GABA (γ -aminobutyric acid) synaptic transmission plays an important role in the construction of developing neuronal circuitry as well as sculpting the activity in the adult brain. Early in development GABAergic synapses are formed before glutamate neurotransmission appears. During this stage the activity of the GABAergic synapses is excitatory due to high intracellular concentration of chloride ion, promoting neural growth and synapse formation [1, 2]. For example, fluorometric recordings of spontaneous calcium ion transients show synchronous and oscillatory wave patterns in the CA1 region of the hippocampus during specific stages of postnatal development [10]. These studies suggest that the role and properties of the GABAergic synapses change as the circuit matures. At the same time, synchronous pattern formation is one of the most prominent neural activity processes observed during development. To date there have been a limited number of theoretical studies addressing the interplay between neuronal synchronization and the changes of GABAergic synaptic properties.

In general, it is believed that synchronization of normal brain rhythms is not realized by excitation alone, but depends critically on synaptic inhibition [3, 13, 20, 22]. However, largely synchronous oscillations are seen in developing neuronal circuits even when GABAergic synapses

*Email address: jeonghy@gatsby.ucl.ac.uk

are depolarising. This appears to be at odds with the previous theoretical prediction that excitatory synapses would cause cortical neurons to become desynchronized (provided that cortical neurons are described as type I membrane dynamics) [6, 9, 12]. The results of Ermentrout and colleagues [4, 7] give a partial explanation for the conditions under which such neurons can synchronize through excitation. The key is the slow voltage-dependent potassium current (M-type) that has the ability to shift a neuron from a type I oscillator to a type II, for which excitation leads to stabilized synchrony. In addition, the calcium-dependent potassium current producing the afterhyperpolarization (AHP) current gives rise to synchronization by making neurons insensitive to inputs that would normally desynchronise the circuit. However, these studies do not show how fluctuations in the reversal potential of the GABAergic synapses affect the synchronization properties or how a large neuronal network acts in the parameter regions treated by the analysis of two neurons. To address these questions we consider three representative regimes of the GABA synapse in reciprocally coupled neuronal circuits: inhibitory, shunting and depolarizing. For these regimes we investigate how the adaptation current affects synchrony. Through both the theoretical analysis and numerical simulations, we finally show that adaptation-induced low firing rates with depolarizing GABA-mediated synapses may be the key to the formation of developing neural circuits through synchronization.

II. THE MODEL AND METHODS

For the neuron model, we use a simplified (1-compartment) conductance-based model due to Traub *et al* [19], consisting of transient sodium, a delayed rectifier, a leak current, and a spike-dependent AHP current which gives spike frequency adaptation without changing the bifurcation structure of the membrane model. Inclusion of such current is warranted since in the early postnatal weeks cortical neurons exhibit long-lasting AHP currents at low spontaneous firing rates [16]. Exact equations and their parameter values are as in the paper of Ermentrout *et al* [7] unless stated differently below.

A first-order kinetic model [5] for the synaptic current represents the transitions between the open and closed state of the GABA receptors. If S is defined as a fraction of the receptors in the open state, it can be described by

$$\frac{dS}{dt} = \frac{\alpha(1-S)}{1 + \exp(-(V_{pre} + 10)/10)} - \beta S, \quad (1)$$

where α and β are forward and backward rate constants for GABA receptors, and V_{pre} is the

presynaptic voltage. Note that synapse speeds up as the backward rate constant β increases. The postsynaptic current I_{GABA} is given by

$$I_{GABA}(t) = \bar{g}_{GABA}S(t)(V - E_{GABA}), \quad (2)$$

where \bar{g}_{GABA} is the maximal conductance, E_{GABA} the reversal potential, and V the postsynaptic membrane potential. In Fig. 1, the bifurcation analysis and the frequency diagram as a function of injected current show that the model neuron is characterized by Type I dynamics with the onset of repetitive firing at zero frequency and a saddle-node bifurcation point.

We analyze the stability of phase-locked solutions for two coupled neurons, by a phase reduction technique using the averaging method. It assumes that the coupling is sufficiently weak for each neuron's trajectory to remain close to its intrinsic stable limit cycle [7, 14, 18], which means that synaptic interactions perturb only the relative phase between the coupled neurons. Under this assumption, a T-periodic averaged interaction function H of phase difference ϕ is obtained and is decomposed into the even and odd parts. Since the even part cancels for the case of symmetric coupling, we can use the odd part to examine the stability of phase-locked solutions. The evolution of phase difference ϕ between two neurons is described by

$$\frac{d\phi}{dt} = \bar{g}_{GABA}(H(-\phi) - H(\phi)) \quad (3)$$

$$= -2\bar{g}_{GABA}H_{odd}(\phi). \quad (4)$$

Phase-locked solutions appear at values of ϕ where the averaged interaction function $H_{odd}(\phi)$ crosses the zero axis, and they are stable when the slope $dH_{odd}/d\phi$ is positive. For the biophysical model, the averaged interaction function H is given by

$$H(\phi) = \frac{1}{T} \int_0^T V^*(t)(E_{GABA} - V(t))S(t + \phi)dt, \quad (5)$$

where V^* is the infinitesimal phase response curve (PRC). From this equation, it is anticipated that the synchronous behavior of neurons results from three factors: the type of membrane dynamics, the reversal potential, and the synaptic interaction function $S(\phi)$.

Five Traub neurons mutually coupled with GABAergic synapses (see above) are simulated in order to confirm the analysis in the various parameter regions. In addition, we extend the phase dynamics to a population of globally coupled neurons since we can approximate the periodic function H by using Fourier transforms [17]:

$$\frac{d\theta_i}{dt} = \omega_i + \frac{\bar{g}_{GABA}}{N} \sum_{j=1}^N \tilde{H}(\theta_j - \theta_i), \quad (6)$$

where the function \tilde{H} is approximated from a few Fourier components of the average interaction function (Five components are used here). If the situation is restricted to identical natural frequencies ($\omega_i = \omega$), the frequency ω can be set to any value (for example, 1) without loss of generality. It is convenient to introduce the two order parameters [11] defined by

$$Z_n(t) = \frac{1}{N} \sum_{j=1}^N \exp(ni\theta_j(t)) \quad (n = 1, 2) \quad (7)$$

which characterizes the collective behavior of the N-neurons described by Eq. 6. These global order parameters contain the instantaneous degree of phase synchronization measure by the moduli, r_1 and r_2 of these two complex numbers at time t . When r_n converges to one in time, the network is in the synchronous state, while the complete asynchronous state results when they go to zero. The network with two equal size clusters specifically gives $r_1 = 0$, but $r_2 = 1$. All numerical simulations and bifurcation analysis are done with the XPPAUT software [8].

III. RESULTS

A. Stability changes by the synaptic reversal potential

Fig. 2 demonstrates that a low firing rate can stabilize synchronization when GABAergic synapses are depolarizing. The adaptation current has a predominant effect due to refractoriness that makes neurons insensitive to inputs arriving after a spike, which is represented by the flattened PRC. At 10Hz, for example, the model without AHP current cannot give rise to synchronous behavior. The adaptation current induces neurons to come close to synchronization when the neurons are coupled with depolarizing GABAergic synapses. One can also see that only the stable anti-phase locked solution exists in the shunting region, regardless of adaptation. It means that synchronization does not happen when GABAergic synapses are shunting. Hyperpolarizing GABAergic synapses cause the phase dynamics to have two stable solutions. However, the in-phase solution of the phase dynamics loses stability when synapses become fast. If the bistability of phase-locked solutions holds for a large neuronal network, the system could break into a two-cluster state, as previously suggested before [21]. Note that the neuron model can be regarded as a Type I membrane since the PRC in Fig. 2 is non-negative so that a brief depolarizing injected current does not delay the phase.

B. Effects of synaptic decay time

The synchronous behavior of neurons is also affected by synapse decay time. In Fig. 3, the circuit shows that inhibitory coupling usually leads to anti-phase solutions, but when synapses are slow, the model gives rise to synchronization. In the shunting region where the synaptic reversal potential is nearly equal to the resting potential of the membrane (E_{rest}), anti-phase solutions are always stable, regardless of synaptic decay time. For depolarized coupling in which the driving force is positive, the phase difference tends to zero as the synapses become faster. As suggested by the average interaction function in Eq. 5, the stability of the phase-locked solution is affected by the adaptation current, the reversal potential and the synaptic function. Five neurons are numerically simulated to check if the analysis for two neurons can be successfully applied to greater numbers of neurons (see Fig. 3E), and it is confirmed that three factors influence synchrony in neurons and that the reversal potential plays a crucial role in changing the synchronous properties.

C. Extension to large neuronal network

In order to extend the analysis of two neurons and the numerical simulation results of five neurons to a large neuronal network, we use a globally coupled phase model with 100 neurons derived from the Traub model (see methods). Under conditions for bistable synchronous and asynchronous solutions of two neurons, we expect a large network to break up into cluster-states. Previous results indeed suggested that the network with inhibitory coupling can break up into the cluster states [21], although they did not treat the biologically realistic model.

The results of mutually synchronizing two coupled neurons can be generalized to more complex situations by using the evolution phase model of Eq. 6. If we assume that interactions are homogeneous, the model can be simulated by using the approximate interaction function $\tilde{H}(\phi)$ obtained from the two coupled neurons. Fig. 4 illustrates that excitatory coupling leads to synchronization but inhibitory coupling leads to desynchronization. These synchronous behaviors of large neuronal networks are in good agreement with the two neuron analysis. In addition, we show that 100 neurons have a two-cluster state when they are coupled with inhibitory GABAergic synapses under conditions for bistable phase-locked solutions as predicted by our analysis above. Order parameters, see Eq. 7, effectively capture a synchronous state. When both r_1 and r_2 converge to 0 or 1 together, the neurons are perfectly synchronized or desynchronized, respectively (Fig. 4A or 4B). However, the model has a cluster state when these two quantities go to different values (Fig. 4C).

IV. CONCLUSIONS

We have analyzed circuits and networks of weakly-coupled Traub neurons affected by various factors: the adaptation current, the reversal potential of GABAergic synapse, and the time-scale of the synaptic function. We have found that neurons tend to have a nearly synchronous state when there is a low firing rate involving an adaptation current and fast GABAergic synapses associated with the environment of developing neurons. These results are corroborated with simulations of a five-neuron circuit. In particular, the analysis shows how different synchronous patterns vary according to the synaptic reversal potential, and it suggests that the depolarizing GABAergic synapses in the developing cortical neurons can cause a near-synchronous state.

In addition, we have found that inhibitorily coupled neurons (GABA hyperpolarising) can give rise to synchronous solutions as well as anti-phase solutions coexisting when synapses are sufficiently slow. Since this situation leads to the bistability of the phase model, we predict that a large neuronal network has the potential to develop into a cluster state depending on the initial condition of the phase dynamics. This has been demonstrated through our analysis of a globally connected network using a phase reduction method. Our results begin to explore how the changing properties of the GABAergic synapses, in consort with the intrinsic neuronal properties, may control patterns of activity during development. How such patterns lead to the formation of neural circuitry remains to be a topic for future study.

V. ACKNOWLEDGMENTS

We thank Peter Dayan for his helpful discussions. We thank the anonymous reviewers for pointing us to the order parameter. This work is supported by Gatsby Charitable Foundation.

-
- [1] Y. Ben-Ari, Developing networks play a similar melody. *Trends in Neurosci.* **24** (2001) 353-360.
 - [2] Y. Ben-Ari, Excitatory actions of GABA during development: The nature of the nurture. *Nature Rev. Neurosci.* **3** (2002) 728-739.
 - [3] P. Bush P and T. Sejnowski, Inhibition synchronizes sparsely connected cortical neurons within and between columns in realistic network models. *J Comput Neurosci.* **3(2)** (1996) 91-110.
 - [4] S.M. Crook, B. Ermentrout, and J.M. Bower, Spike frequency adaptation affects the synchronization properties of networks of cortical oscillators. *Neural Comp.* **10** (1998) 837-854.

- [5] A. Destexhe, Z.F. Mainen, and T.J. Sejnowski, Kinetic models of synaptic transmission, in: Methods in neuronal modeling (MIT, Massachusetts, 1998).
- [6] B. Ermentrout, Type I membranes, phase resetting curves, and synchrony. *Neural Comp.* **8** (1996) 979-1001.
- [7] B. Ermentrout, M. Pascal, and B. Gutkin, The effects of spike frequency adaptation and negative feedback on the synchronization of neural oscillators. *Neural Comp.* **13** (2001) 1285-1310.
- [8] B. Ermentrout, Simulating, analyzing, and animating dynamical systems. (SIAM, Philadelphia, 2002).
- [9] W. Gerstner and W. Kistler, Spiking neuron models (Cambridge University Press, Cambridge, 2002).
- [10] O. Garaschuk, E. Hanse and A. Konnerth, Developmental profile and synaptic origin of early network oscillations in the CA1 region of rat neonatal hippocampus. *J. Physiol.* **507** (1998) 219-236.
- [11] D. Hansel, G. Mato, and C. Meunier, Clustering and slow switching in globally coupled phase oscillators. *Phys. Rev. E* **48** (1993) 3470-3477.
- [12] D. Hansel, G. Mato, and C. Meunier, Synchrony in excitatory neural networks. *Neural Comp.* **7** (1995) 307-337.
- [13] D. Hansel, G. Mato, Asynchronous states and the emergence of synchrony in large networks of interacting excitatory and inhibitory neurons. *Neural Comput.* **15(1)** (2003) 1-56.
- [14] Y. Kuramoto, Chemical oscillations, waves, and turbulence (Springer-Verlag, New York, 1984).
- [15] L. Neltner and D. Hansel, On synchrony of weakly coupled neurons at low firing rate. *Neural Comp.* **13** (2001) 765-774.
- [16] M. Pirchio, J.P. Turner, S.R. Williams, E. Asproдини, and V. Crunelli, Postnatal development of membrane properties and δ oscillations in thalamocortical neurons of the cat dorsal lateral geniculate nucleus. *J. Neurosci.* **17** (1997) 5428-5444.
- [17] A. Pikovsky, M. Rosenblum, and J. Kurths, Synchronization: A universal concept in nonlinear sciences. (Cambridge, Cambridge, 2001).
- [18] J. Rinzel and B. Ermentrout, Analysis of neural excitability and oscillations, in: Methods in neuronal modeling (MIT, Massachusetts, 1998).
- [19] R.D. Traub and R. Miles, Neuronal networks of the hippocampus. (Cambridge University Press, New York, 1991).
- [20] C. van Vreeswijk, L.F. Abbott, and G.B. Ermentrout, When inhibition not excitation synchronizes neural firing. *J. Comp. Neurosci.* **1** (1994) 313-321.
- [21] C. van Vreeswijk, Partial synchronization in populations of pulse-coupled oscillators. *Phys. Rev. E* **54** (1996) 5522-5537.
- [22] X.-J. Wang, Neural Oscillations, in: Encyclopedia of cognitive science (MacMillan Reference Ltd, 2003), 272-280.

FIG. 1: Bifurcation diagram and F-I curve for the Traub two-neuron circuit: A) The bifurcation analysis of a Traub neuron shows that the model has a saddle-node (SN) for a bifurcation point when $\bar{g}_{AHP} = 1$ B) The onset of firing rate occurs at the saddle point and its frequency is zero. The neuron fires at an arbitrarily low frequency when the adaptation current is relatively strong ($\bar{g}_{AHP} = 2$). The smooth lines of the firing rate are fitted to the data obtained from each individual injected current (■). Insets illustrate the firing with and without the adaptation current.

FIG. 2: Both GABAergic reversal potential and AHP affect synchrony. The infinitesimal PRC is shown in the left panel and the bifurcation diagrams for phase difference between two neurons as a function of the reversal potential is plotted in the right panel. In the diagram of the phase difference, solid lines denotes stable solutions and dashed lines unstable solutions. The resting potential is marked on each diagram. Here we control the firing rate of the model by changing the injected current. A) 40Hz without adaptation, B) 10Hz without adaptation, and C) 10Hz with adaptation.

FIG. 3: Effects of the synaptic decay time and numerical simulations: A) The shape of S changes according to the backward reaction rate β . When β increases, synapses become faster. Bifurcation diagrams varying the synaptic time scale with β as the control parameter. B) The hyperpolarizing region, C) The shunting region, and D) The depolarizing region of GABAergic synapses. E) Numerical simulation shows that the analysis for two neurons can be successfully applied to five coupled neurons. In the depolarizing GABAergic connection ($E_{GABA} = -20mV$), the model leads to synchronization when synapses are fast sufficiently (top, $\beta = 2$). In contrast, the model gives rise to desynchronization when synapses are slow (bottom, $\beta = 0.1$).

FIG. 4: Synchrony and onset of cluster states in large networks. The average interaction functions \tilde{H} (solid line) approximated from the two-neuron phase model (dotted line) are plotted in the left panel. With five components in the Fourier transform, we obtain the compatible results with the two-neuron analysis. The evolution of the moduli r_1 and r_2 of the complex order parameters is shown in the right panel. Note that we randomly select the initial condition of network since the cluster-state depends on it. A) $E_{GABA} = 0mV$ with adaptation, B) $E_{GABA} = -80mV$ with adaptation, and C) $E_{GABA} = -80mV$ without adaptation.

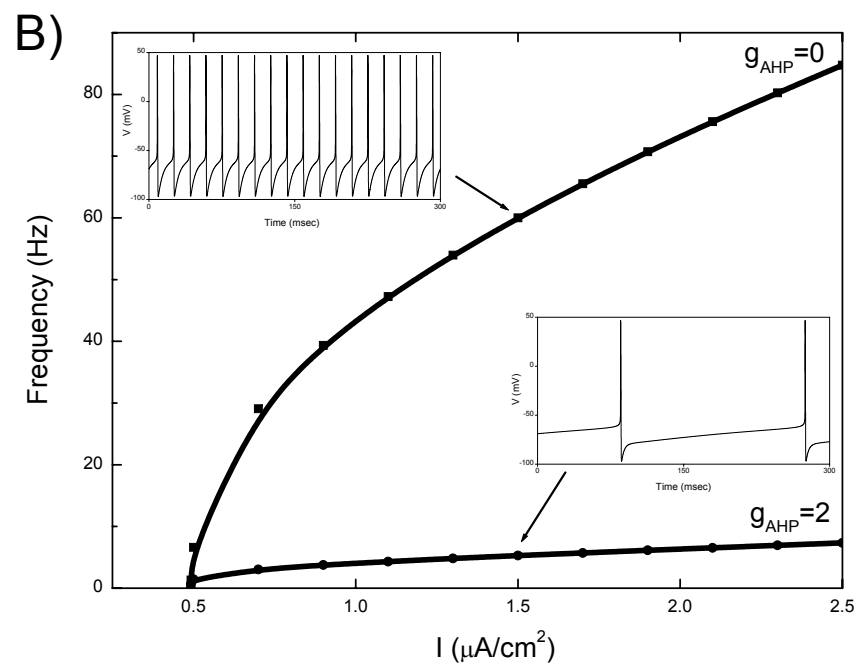
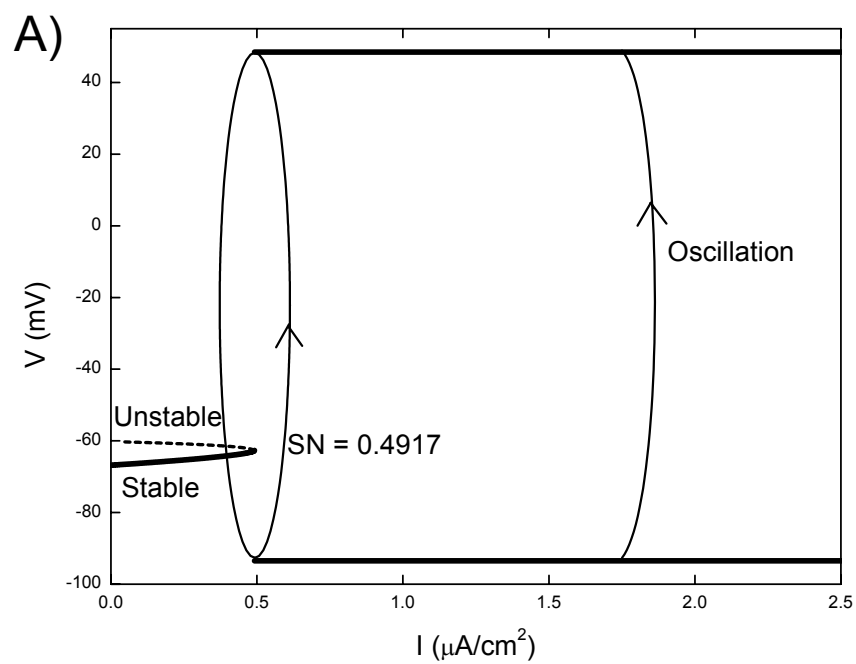


Figure 1 (H.Y. Jeong & B. Gutkin)

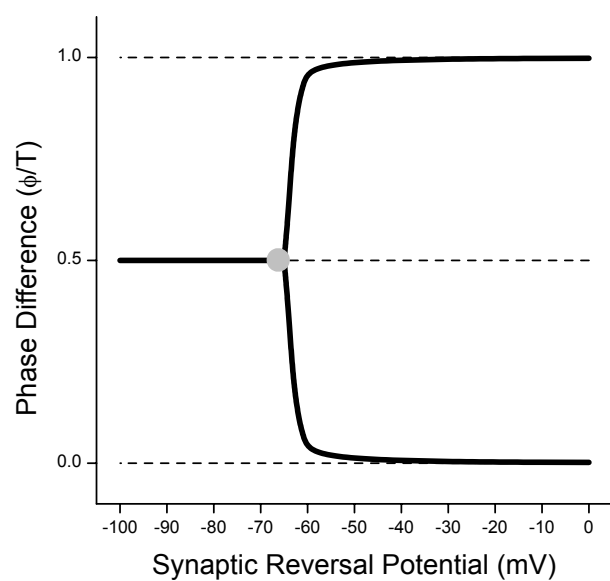
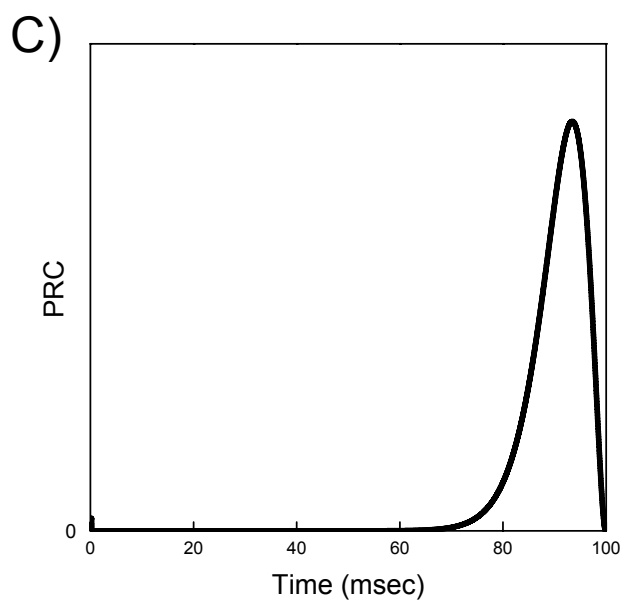
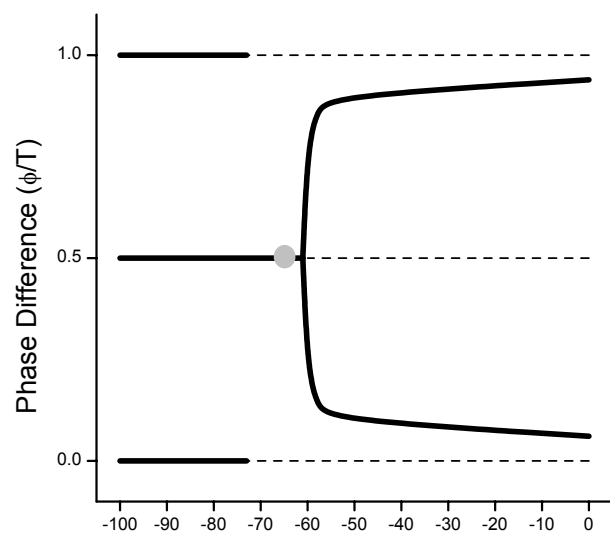
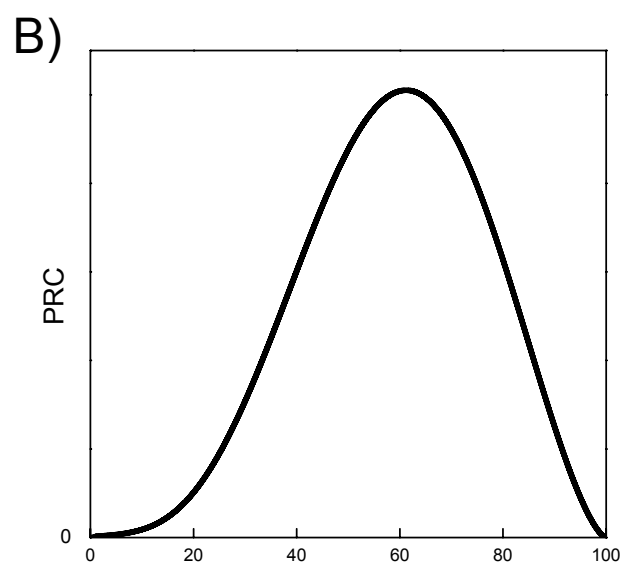
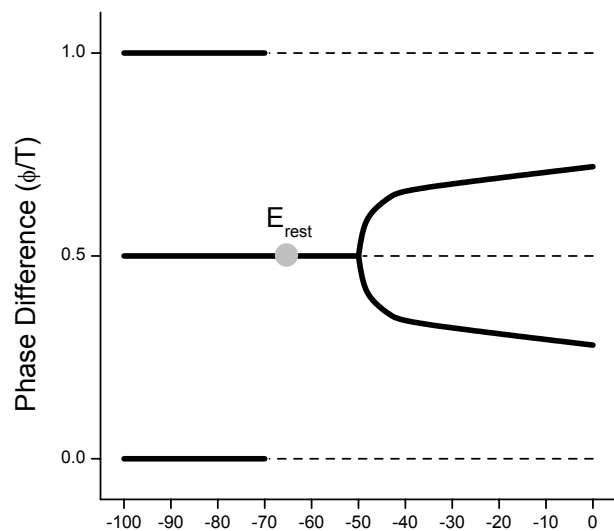
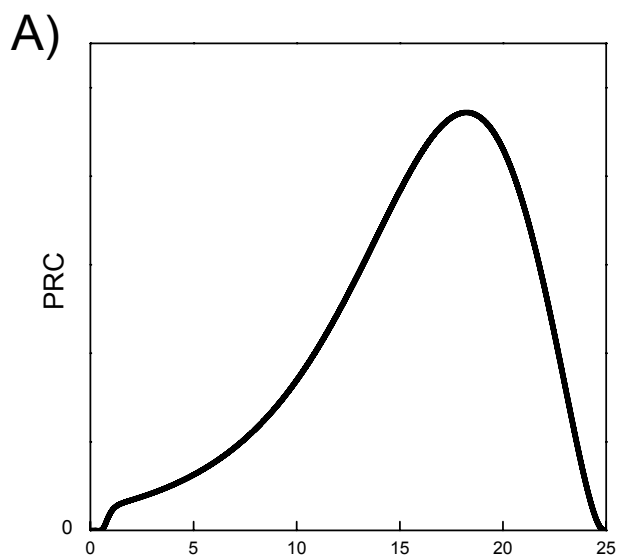


Figure 2 (H.Y. Jeong & B. Gutkin)

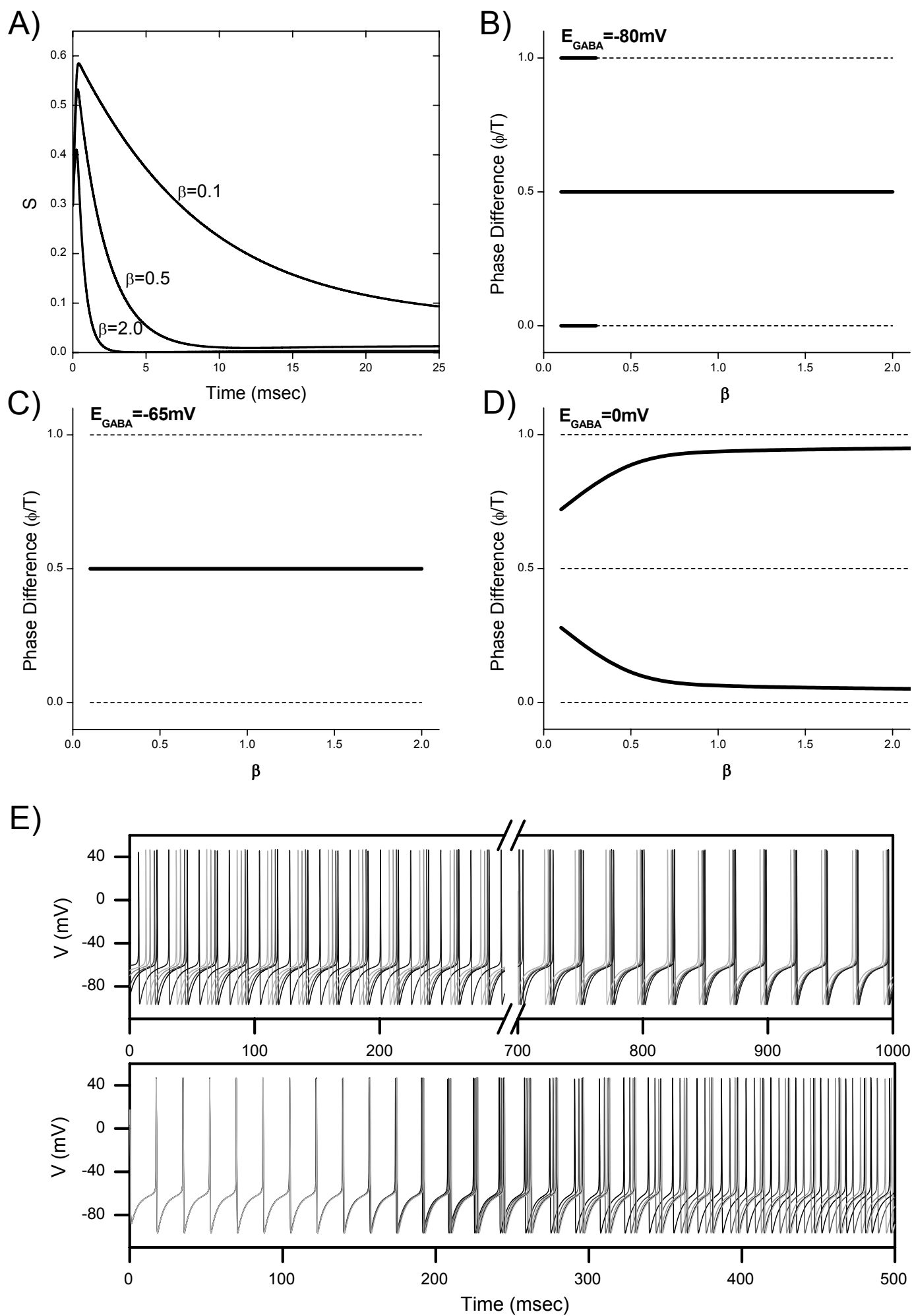


Figure 3 (H.Y. Jeong & B. Gutkin)

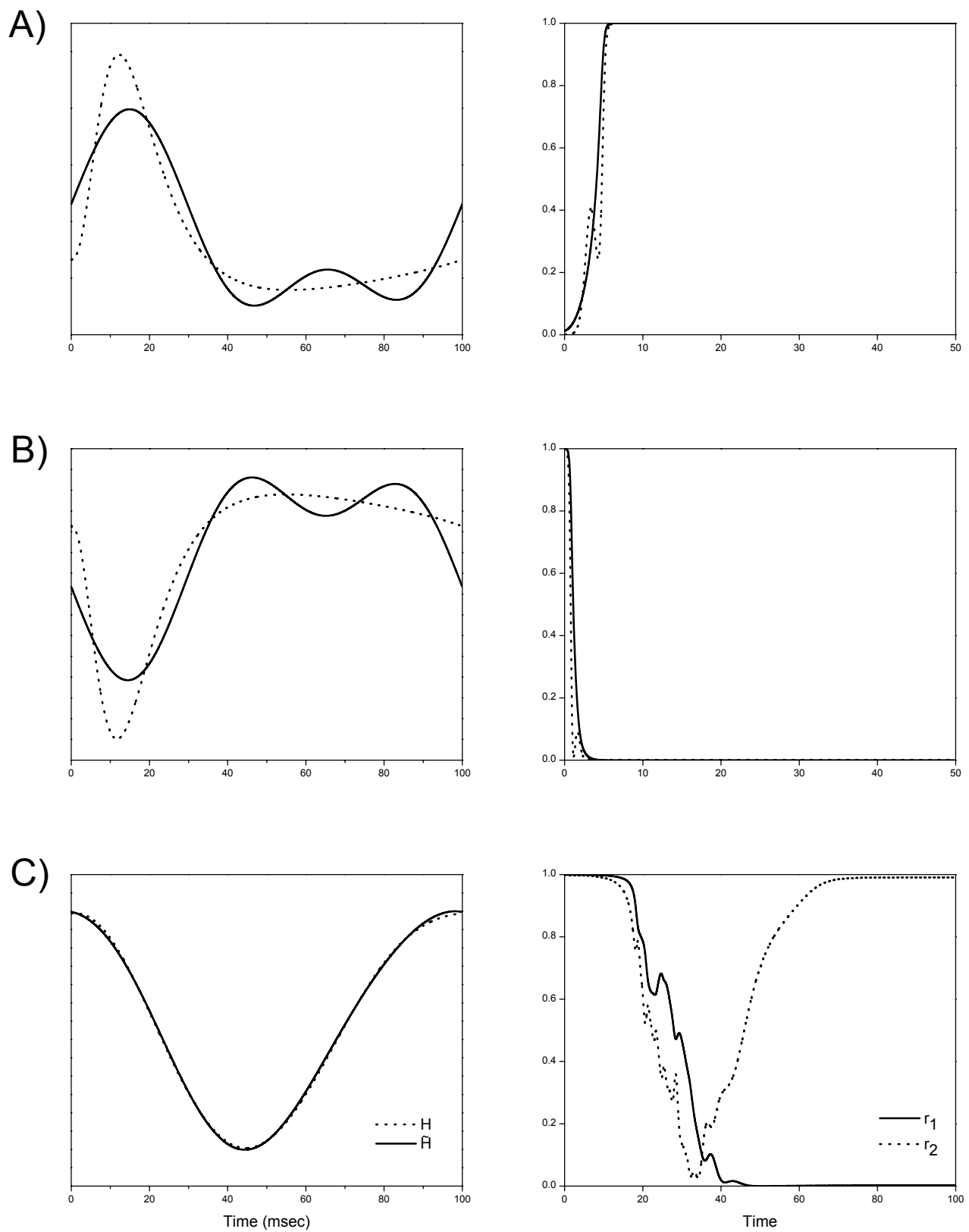


Figure 4 (H.Y. Jeong & B. Gutkin)